



# Functional connectivity disruption of insular subregions in the cirrhotic patients with minimal hepatic encephalopathy

Hong-Yu Lin<sup>1</sup> · Hui-Wei Huang<sup>1</sup> · Qiu-Yi Dong<sup>1</sup> · Li-Min Cai<sup>1</sup> · Hua-Jun Chen<sup>1,2</sup>

Accepted: 11 February 2024 / Published online: 26 February 2024

© The Author(s), under exclusive licence to Springer Science+Business Media, LLC, part of Springer Nature 2024

## Abstract

We investigated abnormal functional connectivity (FC) patterns of insular subregions in patients with minimal hepatic encephalopathy (MHE) and examined their relationships with cognitive dysfunction using resting-state functional magnetic resonance imaging (fMRI). We collected resting-state fMRI data in 54 patients with cirrhosis [20 with MHE and 34 without MHE (NHE)] and 25 healthy controls. After defining six subregions of insula, we mapped whole-brain FC of the insular subregions and identified FC differences through three groups. FC of the insular subregions was correlated against clinical parameters (including venous blood ammonia level, Child-Pugh score, and cognitive score). The discrimination performance between the MHE and NHE groups was evaluated by performing a classification analysis using the FC index. Across three groups, the observed FC differences involved four insular subregions, including the left-ventral anterior insula, left-dorsal anterior insula, right-dorsal anterior insula, and left-posterior insula ( $P < 0.05$  with false discovery rate correction). Moreover, the FC of these four insular subregions progressively attenuated from NHE to MHE. In addition, hypoconnectivity of insular subregions was correlated with the poor neuropsychological performance and the evaluated blood ammonia levels in patients ( $P < 0.05$  with Bonferroni correction). The FC of insular subregions yielded moderate discriminative value between the MHE and NHE groups (AUC = 0.696–0.809). FC disruption of insular subregions is related to worse cognitive performance in MHE. This study extended our understanding about the neurophysiology of MHE and may assist for its diagnosis.

**Keywords** Minimal hepatic encephalopathy · Insula · Cognition · Resting-states functional magnetic resonance imaging · Functional connectivity

## Introduction

Minimal hepatic encephalopathy (MHE) is the first stage of hepatic encephalopathy (HE). This neurological syndrome occurs in patients with cirrhosis (Stinton & Jayakumar, 2013), with a prevalence of 30% ~ 84% (Mina et al., 2014). Although patients with MHE do not have recognizable clinical symptoms of HE, they experience mild cognitive

deficits, such as impairments in visuospatial perception, response inhibition, attention, and delayed information processing (Dhiman & Chawla, 2009). The cognitive dysfunction in MHE negatively affects the patients' ability to perform daily life activities that require attention or fine coordination (e.g., driving vehicles) (Felipo, 2013), and contributes to poor work performance (Ortiz et al., 2005). In fact, MHE leads to social and economic burden for health providers and care givers (Agrawal et al., 2015). In addition, MHE has the potential to progress into overt hepatic encephalopathy, worsening the prognosis and increasing the risk of overall mortality (Moran et al., 2021). The early diagnosis and treatment of patients with MHE can enhance quality of life and improve lifespan as well as slow the progression of neurological impairments (Felipo, 2013). Therefore, it is essential to further elucidate the mechanism underlying MHE, which contributes to the identification of

Hong-Yu Lin, Hui-Wei Huang and Qiu-Yi Dong contributed equally to this work.

✉ Hua-Jun Chen  
chj0075@126.com

<sup>1</sup> School of Medical Imaging, Fujian Medical University, Fuzhou 350001, China

<sup>2</sup> Department of Radiology, Fujian Medical University Union Hospital, Fuzhou 350001, China

diagnostic biomarkers and early preventative treatments (Cheng et al., 2021).

Located deep within the lateral sulcus of the brain, the insula is a critical hub of the brain network (Uddin et al., 2017). It includes several subregions that are involved in distinct functions, such as response inhibition, decision making, attention, and interoception (Uddin et al., 2017). To date, studies using functional magnetic resonance imaging (fMRI) have identified three insular subregions that have distinct patterns of functional connectivity (FC) (Deen et al., 2011): (1) the ventral anterior insula (vAI), the dorsal anterior insula (dAI), and the posterior insula (PI). The vAI is primarily connected with pregenual anterior cingulate cortex and limbic cortex and is involved in cognitive control (Wang et al., 2022). The dAI has primary connections with frontal, anterior cingulate, and parietal areas, and is essential in high-level cognitive processes, including response inhibition and attention (Nomi et al., 2016). The PI has primary connections with parietal and posterior temporal areas and is associated with interoception (Tian & Zalesky, 2018). In fact, the insula can be subdivided into three cytoarchitectonic regions: an agranular region of vAI, a dysgranular region of dAI, and a granular region of PI. These subdivisions reflect a gradual change in cytoarchitectonic complexity in insular cortex (Mesulam & Mufson, 1982).

Insular impairment in MHE has been shown consistently in previous studies (Bajaj et al., 2010). For example, one MHE study histopathologically showed neuronal degeneration and cell death in the insula (Butterworth, 2007). A previous in vivo neuroimaging study based on diffusion kurtosis imaging reported that the microstructural complexity in the insular cortex (especially the right insula) was decreased in patients with cirrhosis and MHE (Chen et al., 2017). Furthermore, the resting-state fMRI study has demonstrated that functional connectivity density in right insula was decreased in patients with MHE (Cheng et al., 2021). In addition, a  $^{18}\text{F}$ -fluorodeoxyglucose positron emission tomography study demonstrated a decrease in glucose utilization in the right insula of patients with MHE (Zhang et al., 2019). Collectively, the insula represents a critical pathological node of MHE, exhibiting structural, functional, and metabolic abnormalities that are associated with reduced

performance in cognitive processes, such as execution and attention (Chen et al., 2017; Cheng et al., 2021; Zhang et al., 2019).

FC alterations have been widely described in MHE (Zhang et al., 2014). One study used resting-state fMRI and found that cirrhotic patients with MHE suffered from disrupted FC, which involved the anterior cingulum gyrus, thalamus, and frontal cortex (Ni et al., 2012). The decreased basal ganglia–thalamo-cortical FC was also found in patients with MHE (Zhang et al., 2012). Furthermore, in patients with MHE, FC reduction has been observed in multiple brain intrinsic networks, including the default mode and dorsal attention networks. In addition, the progressive impairment of dynamic FC has been identified as the MHE disease advances (Lin et al., 2021). These FC changes correspond to the severity of cognitive dysfunctions, including visuo-motor slowing, deficits of cognitive control, and attention decline (Lin et al., 2021; Ni et al., 2012; Qi et al., 2012a; Qi, Zhang, Xu, Qi et al., 2012a, b, c). In spite of these efforts, however, changes in the insular FC among patients with MHE have not been fully clarified. Therefore, in this study, we investigated abnormal FC patterns of insular subregions in patients with MHE using resting-state fMRI and examined their relationships with cognitive dysfunction.

## Materials and methods

### Subjects

The Research Ethics Committee of Fujian Medical University Union Hospital, China, approved this study. Before inclusion in the study, all participants provided written informed consent. The participants recruited for this study included 54 patients with cirrhosis [20 with MHE, 34 without MHE (NHE)] and 25 healthy control (HC) subjects. Table 1 provides the clinical and demographic information for the participants. On the basis of the psychometric hepatic encephalopathy score (PHES) examination, we diagnosed patients with MHE (who have PHES < -4 points). We used the PHES examination, which includes number connection tests A and B, a digit symbol test, line tracing test, and serial

**Table 1** Clinical and demographic characteristics of participants

MHE, minimal hepatic encephalopathy; NHE, cirrhotic patients without MHE; HC, healthy controls; HBV, hepatitis B virus

	HC group	NHE group	MHE group	P value
Age (years)	54.60 ± 7.90	55.71 ± 10.49	53.65 ± 9.44	0.736
Sex (male/female)	19/6	28/6	16/4	0.835
Years of education	6.40 ± 2.24	6.38 ± 3.37	6.05 ± 4.17	0.924
Etiology of cirrhosis (HBV/Alcoholism/HBV and alcoholism/Cryptogenic)	-	19/3/7/5	16/3/1/0	-
Child-Pugh score	-	6.88 ± 1.89	7.85 ± 2.06	-
Blood ammonia level (μmol/L)	-	29.49 ± 15.7	40.99 ± 26.45	-
Psychometric Hepatic Encephalopathy Score	0.40 ± 1.44	-0.06 ± 1.67	-7.00 ± 3.09	< 0.001

dotting test, to assess neurocognitive function. PHES test, which is widely used as the “gold standard” for the diagnosis of MHE, is discussed in other work (Chen et al., 2015).

The criteria for exclusion were (1) diagnosis of a neuropsychiatric disorder such as current overt hepatic encephalopathy (defined by West Haven criteria (Ferenci et al., 2002), Alzheimer’s disease, and Parkinson disease, (2) currently being treated with psychotropic drugs, (3) current diagnosis of an uncontrollable endocrine or metabolic disorder (e.g., thyroid dysfunction), and (4) alcohol abuse within the six months before the study.

### MRI data acquisition

We acquired MRI data on a 3 T MRI scanner (Siemens, Prisma, Germany). During the resting-state fMRI examination, we asked participants to keep their eyes closed but be awake, hold still, and not to think of anything in particular. To reduce the head motion of participants, we used a foam pad. We used three-dimensional T1-weighted magnetization-prepared rapid gradient echo (MPRAGE) images, which we gathered according to the following parameters: repetition time (TR)=1610 ms, echo time (TE)=2.25 ms, field of view (FOV)=224 mm × 224 mm, matrix=224×224, flip angle=8°, slice thickness=1.0 mm, and 176 sagittal slices. To capture resting-state functional images, we used the multiband slice acquisition technique. The parameters for the echo-planar imaging sequence were as follows: multiband factor=4, TR=700 ms, TE=30 ms, acquisition matrix=76×76, FOV=228 mm × 228 mm, flip angle=50°, 48 axial slices, slice thickness=3 mm (no interslice gap), and 600 volumes.

### MRI data processing

We performed data preprocessing using the Data Processing and Analysis for Brain Imaging tool (DPABI v6.0, <http://rfmri.org/dpabi>) and included the following steps: (1) discarding the initial 30 volumes; (2) realignment; (3) spatial normalization; (4) smoothing with 4 mm Gaussian kernel; (5) linear detrend; (6) temporal filtering (0.01–0.08 Hz); and (7) regressing out nuisance covariates, including the estimated motion parameters based on the Friston-24 model and the mean signals of the cerebrospinal fluid, white matter, and global brain.

We conducted the seed-based connectivity analyses for six insular subregions, including left and right ventral anterior insula (L-vAI and R-vAI), left and right dorsal anterior insula (L-dAI and R-dAI), and left and right posterior insula (L-PI and R-PI) (Deen et al., 2011). The six spherical (radius=6 mm) centered on these insular subregions were taken as seeds, whose given MNI coordinates were as

follows: L-vAI (−33, 13, −7), R-vAI (32, 10, −6), L-dAI (−38, 6, 2), R-dAI (35, 7, 3), L-PI (−38, −6, 5), and R-PI (35, −11, 6). For each seed, we generated an individual FC map by calculating Pearson’s correlation coefficients between the mean time series of this seed and the time series of all other voxels within the entire brain. Thereby, six FC maps were generated for each subject. To enhance normality, we normalized the individual correlation map to z-map by using Fisher’s Z transformation.

### Statistical analysis

The statistical module in DPABI software was adopted for the analyses about FC. For every group, the z-maps were entered into a random effect one-sample *t*-test to determine the regions that presented significant connectivity with each insular subregion seed. The threshold was set at  $P < 0.01$  and was corrected by the false discovery rate (FDR) approach. Then, we extracted and combined the FC maps of each insular subregion in three groups to produce the masks for the subsequent intergroup comparison. To determine the intergroup difference in FC of each insular subregion, we performed Analysis of Variance (ANOVA) in a voxel-wise manner, controlling for the sex, age, and year of education. The multiple comparisons were corrected by FDR approach and the threshold was set at  $P < 0.05$ . After that, we selected the areas showing significant intergroup difference in FC as the regions of interests (ROIs), which we used for the subsequent analyses.

For each ROI, we calculated its FC strength with insular subregion seed and correlated it against clinical parameters (including venous blood ammonia level, Child-Pugh score that reflects hepatic function, and PHES that reflects cognition level) using the Pearson correlation analysis among the cirrhotic patients. The statistical significance level was set at  $P < 0.05$  (with Bonferroni correction). For each ROI, we used its FC strength with insular subregion seed as the indices for the receiver operating characteristic (ROC) curve analysis. We estimated the area under the ROC curve (AUC) to evaluate the discrimination performance between NHE and MHE group. The statistical threshold was set at  $P < 0.05$ . The above statistical processes were conducted using the SPSS 22.0 software (SPSS, Inc., Chicago, IL, USA).

## Results

### Participant demographics and PHES performance

The clinical and demographic characteristics of the participants are given in Table 1. Among the three groups, we did

not observe any significant differences in sex ( $P=0.835$ ), age ( $P=0.736$ ), or years of education ( $P=0.924$ ). Compared with HC and NHE groups (both  $P<0.001$ ), patients with MHE had lower PHES, which suggest significantly worse neurocognitive performance.

### Within-group FC of the insular subregions

Figure 1 illustrates the FC pattern of insular subregions within the three groups. In HC, the vAI has predominant functional connection with the insula, rolandic operculum, superior frontal gyrus (dorsolateral part), middle frontal

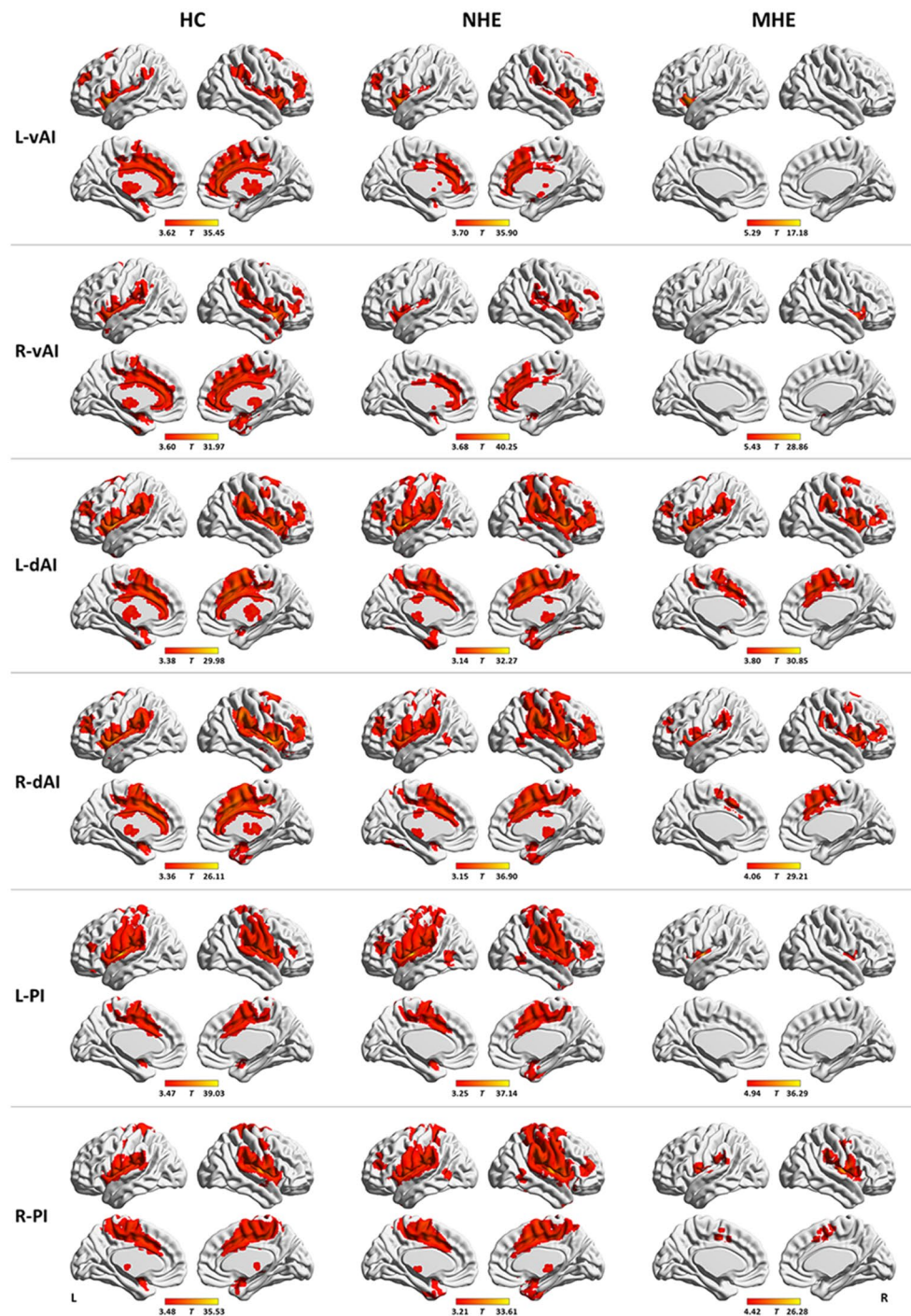


**Fig. 1** Functional connectivity pattern of insular subregions within three groups. MHE, minimal hepatic encephalopathy; NHE, cirrhotic patients without MHE; HC, healthy controls; L, left; R, right; L-vAI

and R-vAI, left and right ventral anterior insula; L-dAI and R-dAI, left and right dorsal anterior insula; L-PI and R-PI, left and right posterior insula



gyrus, inferior frontal gyrus (opercular part), supplementary motor area, anterior cingulate and paracingulate gyrus, median cingulate and paracingulate gyrus, supramarginal gyrus, superior temporal gyrus, temporal pole, and putamen. The dAI showed functional connectivity primarily with the insula, rolandic operculum, middle frontal gyrus, inferior frontal gyrus (opercular and triangular part), supplementary motor area, precentral gyrus, anterior cingulate and paracingulate gyrus, median cingulate and paracingulate gyrus, supramarginal gyrus, superior temporal gyrus, temporal pole, putamen, and thalamus. The PI exhibited functional connectivity primarily with the insula, rolandic operculum, supplementary motor area, paracentral lobule, precentral gyrus, postcentral gyrus, median cingulate and paracingulate gyrus, supramarginal gyrus, precuneus, angular gyrus, superior temporal gyrus, temporal pole, and putamen. Relative to HC, NHE patients exhibited similar FC patterns of insular subregions, whereas patients with MHE displayed reduced FC extent and strength (see below).

### Intergroup differences in FC of the insular subregions

As shown in Table 2; Fig. 2, we observed significant differences in FC of four insular subregions across three groups (FDR corrected  $P < 0.05$ ). These differences involved the FC between L-vAI seed and the ROI 1–2 (ROI 1, bilateral anterior and middle cingulate gyrus and medial frontal gyrus; ROI 2, bilateral middle and posterior cingulate gyrus). These observed differences also included the FC between L-dAI seed and the ROI 3–4 (ROI 3, right insula and superior temporal gyrus; ROI 4, bilateral anterior and middle cingulate gyrus). In addition, intergroup differences involved the FC between R-dAI seed and the ROI 5–9 (ROI 5, left insula and superior temporal gyrus; ROI 6,

left insula and superior temporal gyrus; ROI 7, right insula and superior temporal gyrus; ROI 8, bilateral middle and anterior cingulate gyrus; ROI 9, right supramarginal gyrus). The FC between L-PI seed and the ROI 10–11 (ROI 10, left insula, postcentral gyrus, and superior temporal gyrus; ROI 11, right insula, postcentral gyrus, and superior temporal gyrus) also revealed intergroup differences. Additionally, we observed progressive reductions in FC from NHE to MHE.

### Results of correlation analysis

The FC between the L-vAI and the ROI 1 exhibited a positive correlation with the PHES among the cirrhotic patients (Table 3). There was also a positive correlation with PHES and the connectivity joining L-dAI and the ROI 3–4. Moreover, the PHES showed a correlation with the FC between the R-dAI and the ROI 7–9, as well as the FC between the L-PI and the ROI 11 ( $P < 0.05$  with Bonferroni correction).

Additionally, we found the higher blood ammonia level to be significantly correlated with decreased FC of insular subregions, including the FC between the L-dAI and the ROI 3 as well as the FC between the R-dAI and the ROI 6–7 ( $P < 0.05$  with Bonferroni correction) (Table 3). Also, the blood ammonia level was significantly correlated with the FC between the L-PI and the ROI 10 in cirrhotic patients. There was no correlation ( $P > 0.05$  after Bonferroni correction), however, between the Child-Pugh score and the FC of insular subregions.

### Diagnostic performance based on ROC analysis

Several FC measures showed the discriminant potential between NHE and MHE, including the FC between L-vAI and ROI 1, the FC between L-dAI and ROI 3, the FC

**Table 2** Brain regions showing significant intergroup difference in FC of insular subregion

ROI index	Seed	Brain regions	Cluster size (voxel)	Brodmann area	MNI coordinates			Peak <i>F</i> value
					<i>x</i>	<i>y</i>	<i>z</i>	
ROI 1	L-vAI	Bilateral anterior and middle cingulate gyrus and medial frontal gyrus	262	32/24/9	0	15	39	14.71
ROI 2	L-vAI	Bilateral middle and posterior cingulate gyrus	52	24/31	−3	−12	39	11.66
ROI 3	L-dAI	Right insula and superior temporal gyrus	51	13/22	45	3	−3	12.97
ROI 4	L-dAI	Bilateral anterior and middle cingulate gyrus	54	32/24	−3	18	30	12.33
ROI 5	R-dAI	Left insula and superior temporal gyrus	85	13/22	−42	−15	−6	13.36
ROI 6	R-dAI	Left insula and superior temporal gyrus	181	13/22	−42	3	3	16.61
ROI 7	R-dAI	Right insula and superior temporal gyrus	297	13/22	45	3	0	14.73
ROI 8	R-dAI	Bilateral middle and anterior cingulate gyrus	204	24/32	−3	18	30	15.74
ROI 9	R-dAI	Right supramarginal gyrus	184	40	60	−36	39	10.30
ROI 10	L-PI	Left insula, postcentral gyrus, and superior temporal gyrus	69	13/43/22	−48	−9	12	10.59
ROI 11	L-PI	Right insula, postcentral gyrus, and superior temporal gyrus	117	13/42/43	45	−24	18	15.01

ROI, regions of interest; L-vAI and R-vAI, left and right ventral anterior insula; L-dAI and R-dAI, left and right dorsal anterior insula; L-PI and R-PI, left and right posterior insula

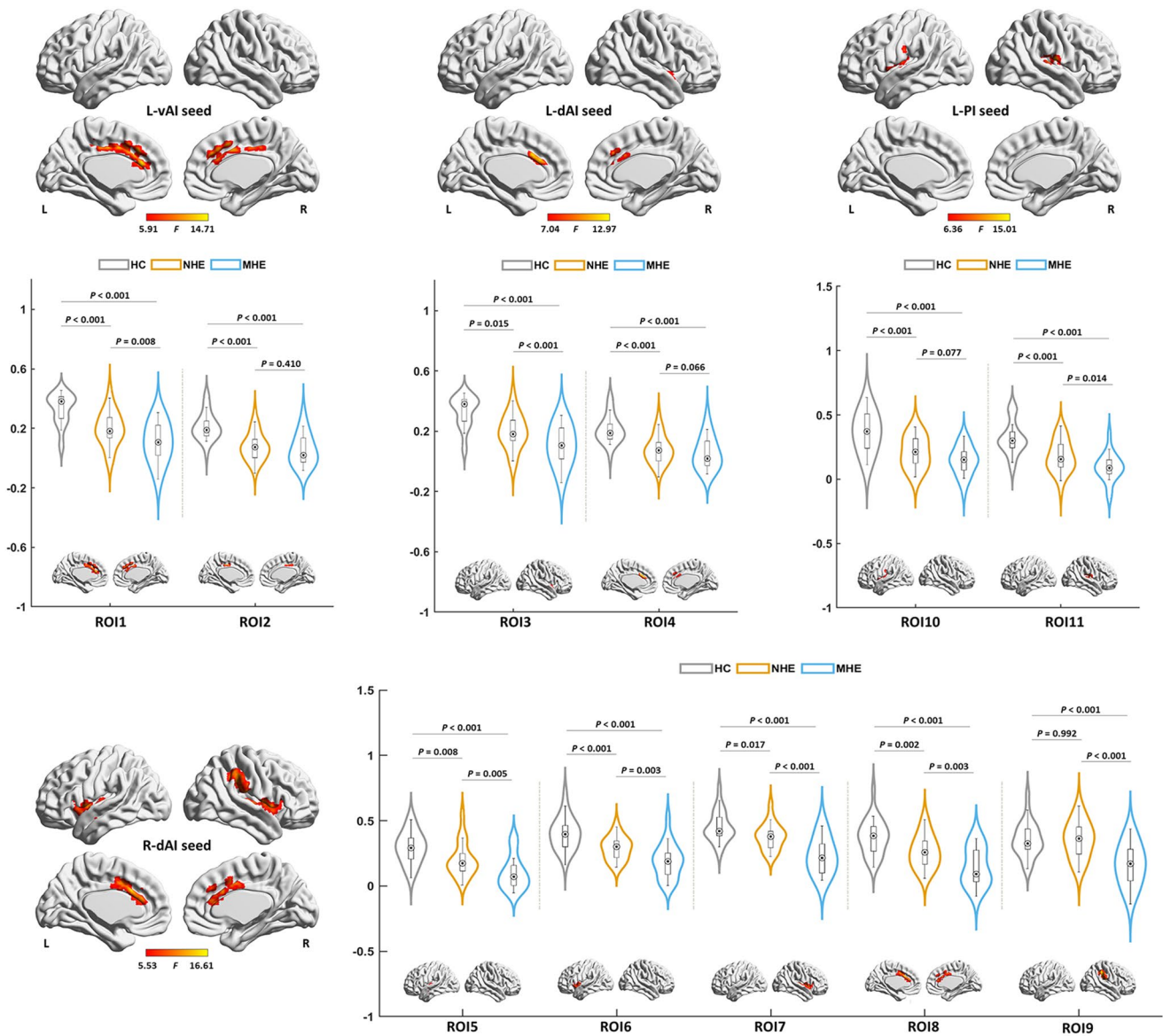


**Fig. 2** The intergroup differences in functional connectivity of insular subregions. Violin and box plots depict the intergroup differences and distribution of functional connectivity. MHE, minimal hepatic encephalopathy; NHE, cirrhotic patients without MHE; HC, healthy

controls; L, left; R, right; L-vAI, left ventral anterior insula; L-dAI and R-dAI, left and right dorsal anterior insula; L-PI, left posterior insula. The regions with functional connectivity differences are shown in red color. The details of ROIs see Table 2

between R-dAI and ROI 5–9, and the FC between L-PI and ROI 11 (Fig. 3; Table 4). The corresponding AUC ranged from 0.696 to 0.809; and the  $P$  values varied between less than 0.001 and 0.017. In contrast, the FC between the L-vAI and ROI 2 (AUC = 0.588,  $P = 0.282$ ), the FC between the L-dAI and ROI 4 (AUC = 0.660,  $P = 0.051$ ), and the FC between the L-PI and ROI 10 (AUC = 0.640,  $P = 0.089$ ) showed no significant potential in distinguishing between these two groups.

controls; L, left; R, right; L-vAI, left ventral anterior insula; L-dAI and R-dAI, left and right dorsal anterior insula; L-PI, left posterior insula. The regions with functional connectivity differences are shown in red color. The details of ROIs see Table 2

## Discussion

This study represents a pioneering effort in applying resting-state FC analysis to detect functional synchronization between the insular subregions and the whole brain in MHE. The findings are as follows: (1) The observed FC differences involved four insular subregions, including the L-vAI, L-dAI, R-dAI, and L-PI. (2) The FC of these four insular subregions were progressively attenuated from NHE to MHE. (3) According to the FC, the insular subregion function was negatively correlated with blood ammonia levels and positively correlated with cognitive performance.

**Table 3** Correlation coefficient between clinical parameters and functional connectivity of insular subregion

ROI index	Seed	Blood ammonia level ( $\mu\text{mol/L}$ )	Child-Pugh score	PHES
ROI1	L-vAI	-0.300 ( <b><math>P=0.028</math></b> )	-0.120 ( $P=0.388$ )	0.487 ( <b><math>P&lt;0.001</math></b> )*
ROI2	L-vAI	-0.174 ( $P=0.207$ )	0.063 ( $P=0.651$ )	0.171 ( $P=0.217$ )
ROI3	L-dAI	-0.418 ( <b><math>P=0.002</math></b> )*	-0.231 ( $P=0.092$ )	0.518 ( <b><math>P&lt;0.001</math></b> )*
ROI4	L-dAI	-0.267 ( $P=0.051$ )	-0.082 ( $P=0.555$ )	0.381 ( <b><math>P=0.005</math></b> )*
ROI5	R-dAI	-0.307 ( <b><math>P=0.024</math></b> )	-0.081 ( $P=0.561$ )	0.379 ( <b><math>P=0.005</math></b> )
ROI6	R-dAI	-0.417 ( <b><math>P=0.002</math></b> )*	-0.201 ( $P=0.145$ )	0.358 ( <b><math>P=0.008</math></b> )
ROI7	R-dAI	-0.510 ( <b><math>P&lt;0.001</math></b> )*	-0.130 ( $P=0.347$ )	0.491 ( <b><math>P&lt;0.001</math></b> )*
ROI8	R-dAI	-0.373 ( <b><math>P=0.005</math></b> )	-0.164 ( $P=0.237$ )	0.407 ( <b><math>P=0.002</math></b> )*
ROI9	R-dAI	-0.311 ( <b><math>P=0.022</math></b> )	-0.098 ( $P=0.479$ )	0.426 ( <b><math>P=0.001</math></b> )*
ROI10	L-PI	-0.385 ( <b><math>P=0.004</math></b> )*	-0.311 ( <b><math>P=0.022</math></b> )	0.347 ( <b><math>P=0.010</math></b> )
ROI11	L-PI	-0.284 ( <b><math>P=0.038</math></b> )	-0.291 ( <b><math>P=0.033</math></b> )	0.399 ( <b><math>P=0.003</math></b> )*

ROI, regions of interest; L-vAI and R-vAI, left and right ventral anterior insula; L-dAI and R-dAI, left and right dorsal anterior insula; L-PI and R-PI, left and right posterior insula; PHES, Psychometric Hepatic Encephalopathy Score. Bold indicates  $P$  value  $<0.05$ . The symbol \* indicates  $P$  value  $<0.05$  with Bonferroni correction. The details of ROIs see Table 2; Fig. 2

(4) The hypoconnectivity of insular subregions emerged as a moderate differentiating index in distinguishing MHE from NHE. The findings of this study verify that insular FC is a promising neuroimaging biomarker for patients with MHE.

Hypoconnectivity of insular subregions in MHE may be associated with the excessive neuroinhibition, which is attributed to the increase in inhibitory neurotransmission (e.g.,  $\gamma$ -amino butyric acid) observed in patients with MHE (Ahboucha et al., 2005; Cauli et al., 2009; Jones, 2000). Another explanation about FC disruption of insular subregions may be associated with the decrease of glucose utilization (Lockwood et al., 2002), which means reduced energy metabolism and negatively affects neurotransmission activities (Keiding & Pavese, 2013). In addition, the neuronal loss of in insula, which can result in the loss of neurotransmission receptor sites and the impairment of the receptor-mediated neural pathway (Butterworth, 2007), may also contribute to hypoconnectivity in patients with MHE (Chen et al., 2012).

The decreased FC observed in the left anterior insula (including the ventral and dorsal parts) in patients with MHE is consistent with the previous findings, which have demonstrated aberrant neural functional activity in the left anterior insula (Qi et al., 2012) and left insular atrophy among cirrhotic patients with MHE (Liu et al., 2019). The vAI and dAI have been shown to be involved in emotion-related tasks (including decision making and emotional working memory) and attention-demanding tasks (Smith et al., 2017). Therefore, one of the neural substrates for MHE-related deficits in working memory, attention, and decision making may be attributed the weaker connectivity of L-vAI and L-dAI (Karanfilian et al., 2020).

Patients with MHE also had a significant reduction in FC of the R-dAI. Previous investigations, aligned with our result, also have identified weaker connectivity and decreased structural complexity in the right anterior insula

(Qi et al., 2012b; Yang et al., 2018). Moreover, it has been proposed that R-dAI, anchored in the salient network, is critical for integrating internal and external stimuli; it further mediates many cognitive processes, including saliency detection, episodic memory consolidation, and attentional capture (Menon & Uddin, 2010). Therefore, abnormal FC of R-dAI may be a possible mechanism underlying the MHE-related impairments in these aforementioned cognitive functions (Karanfilian et al., 2020). According to our findings, the link between poor cognitive performance and the decreased FC of R-dAI in cirrhotic patients supports this speculation.

The present study revealed disturbed FC of L-PI in patients with MHE, which supports previous studies that revealed abnormal neural activity in the posterior insular cortex of patients with MHE (Qi et al., 2012). The FC disruption of the L-PI may indicate relevant abnormalities in motor and sensory functions (Karanfilian et al., 2020), which have been observed in patients with MHE, given that L-PI processes primary sensory information related to motor and somatosensory control (Cauda et al., 2011).

A negative correlation between insular FC disruption and hyperammonemia was identified in cirrhotic patients, which suggested that insular dysfunction may be associated with ammonia neurotoxicity that can disturb the neural communication (Córdoba & Mínguez, 2008; Häussinger & Schliess, 2008). Consistently, several previous investigations have identified the correlation between FC in brain network and the blood ammonia level in the case of cirrhosis (Qi et al., 2014; Qi, Zhang, Xu, Qi et al., 2012a, b, c). In addition, moderate performance has been obtained using insular FC as the index for diagnosing MHE. These results were compatible with earlier studies that showed the promising value of FC measurement in identifying cirrhotic patients with MHE (Lin et al., 2019). Meanwhile, the stepwise attenuation of insular FC was found from NHE to MHE, which

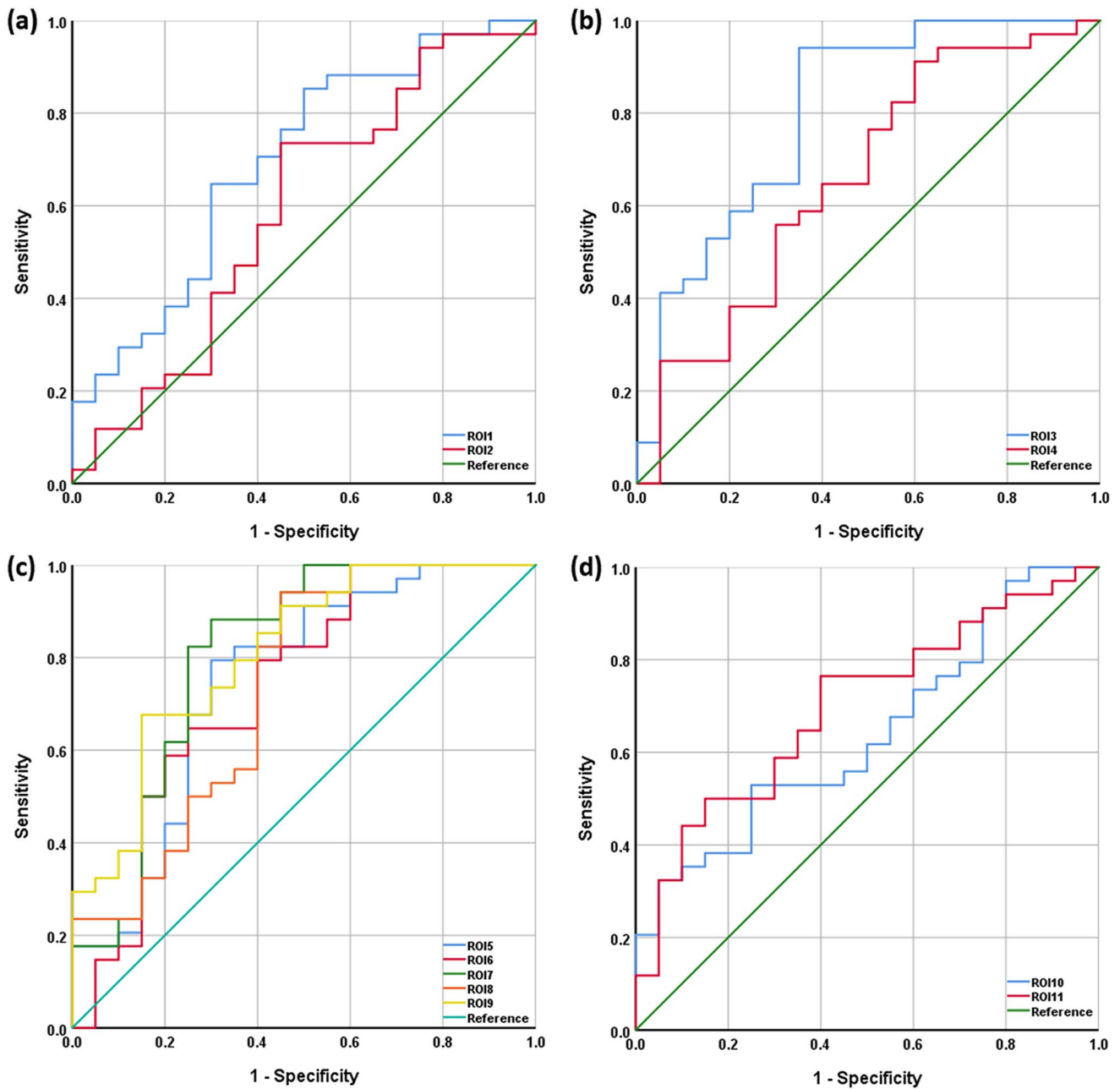


**Fig. 3** The results of receiver operating characteristic curve analysis between NHE and MHE groups. The discrimination indices are functional connectivity of insular subregion seeds: **(a)** left ventral anterior

insula (L-VAI); **(b)** left dorsal anterior insula (L-dAI); **(c)** right dorsal anterior insula (R-dAI); **(d)** left posterior insula (L-PI). The details of ROIs see Table 2; Fig. 2

aligns with previous observations that have shown a progressive FC disruption in brain network with HE disease development (Lin et al., 2019, 2021). Thus, the potential of insular FC measurement severing as the biomarker for diagnosing MHE and monitoring disease development was demonstrated by our study. However, these results may be restricted by relatively small study population; therefore, it would be valuable to conduct further multicenter clinical

investigations with larger sample sizes to further validate these findings.

This study had several limitations. First, we adopted three seeds of insular subregions according to the recommendations derived from previous studies (Deen et al., 2011), to date, however, there is no gold standard on insular parcellation and, therefore, controversial about the optimal number of insula subregions remains (Tian & Zalesky, 2018). Second, this study was cross-sectional. To observe



**Table 4** Area under the receiver operating characteristic curve obtained in the analyses using functional connectivity indices

ROI index	Seed	Area under curve	95% Confidence Interval	<i>P</i> value
ROI1	L-vAI	0.696	0.548–0.843	<b>0.017</b>
ROI2	L-vAI	0.588	0.423–0.754	0.282
ROI3	L-dAI	0.803	0.674–0.932	<b>&lt; 0.001</b>
ROI4	L-dAI	0.660	0.504–0.816	0.051
ROI5	R-dAI	0.747	0.602–0.893	<b>0.003</b>
ROI6	R-dAI	0.734	0.584–0.884	<b>0.004</b>
ROI7	R-dAI	0.806	0.671–0.941	<b>&lt; 0.001</b>
ROI8	R-dAI	0.732	0.584–0.881	<b>0.005</b>
ROI9	R-dAI	0.809	0.688–0.930	<b>&lt; 0.001</b>
ROI10	L-PI	0.640	0.491–0.789	0.089
ROI11	L-PI	0.699	0.557–0.840	<b>0.016</b>

ROI, regions of interest; Bold indicates *P* value < 0.05. The details of ROIs see Table 2; Fig. 2

the insular FC changes after treatment and verify the causal relationship between FC disruption and cognitive dysfunction, a longitudinal study is warranted. Third, because we only used PHES to assess general neurocognitive function, it is necessary to profile more detailed cognition domains in future studies. Fourth, the issue about overfitting should be concerned during assessing diagnostic performance based on ROC analysis, since the ROIs were beforehand selected by intergroup comparison. Meanwhile, an independent dataset is warranted to further validate the diagnostic performance of insular FC measures in the future study. Fifth, the sample size in current study was relatively small, resulting in the limited statistical power and preventing the more comprehensive evaluation about the potential influence of distinct etiology of cirrhosis on the insular FC.

In summary, this study applied resting-states fMRI, for the first time, to explore abnormal FC patterns of insular subregions in patients with cirrhosis and MHE. Our findings suggested that the disturbed insular FC may contribute to poor cognitive performance in MHE and the FC alteration may serve as a promising biomarker for MHE. This study extended our understanding of the pathophysiology of MHE and may assist for its diagnosis.

### Abbreviations

MHE	minimal hepatic encephalopathy
HE	hepatic encephalopathy
fMRI	functional magnetic resonance imaging
FC	functional connectivity
vAI	ventral anterior insula
dAI	dorsal anterior insula
PI	posterior insula
NHE	without minimal hepatic encephalopathy
HC	healthy control
PHES	Psychometric Hepatic Encephalopathy Score

TR	repetition time
TE	echo time
FOV	field of view
L-vAI	left ventral anterior insula
R-vAI	right ventral anterior insula
L-dAI	left dorsal anterior insula
R-dAI	right dorsal anterior insula
L-PI	left posterior insula
R-PI	right posterior insula
FDR	False Discovery Rate
ROIs	regions of interests
ROC	receiver operating characteristic
AUC	area under the ROC curve

**Author contributions** Experimental conception and design were presented by H.C. Material preparation, data collection and analysis were performed by H.C., H.L., H.H., Q.D., and L.C. The first draft of the manuscript was written by H.L. and L.C. The writing review and editing was done by H.C., H.L., H.H., and Q.D. All authors read and approved the final version of the manuscript.

**Funding** This study was funded by the National Natural Science Foundation of China (No. 82071900) and Fujian Province Joint Funds for the Innovation of Science and Technology (No. 2019Y9067).

**Data availability** The data that support the findings of this study are available from the corresponding author upon request.

### Declarations

**Ethical approval** This study was performed in accordance with the principles outlined in the Helsinki Declaration. The Research Ethics Committee of Fujian Medical University Union Hospital, approved this study.

**Consent to participate** Written informed consent was obtained from all subjects (patients) in this study.

**Consent for publication** All authors have read and approved the manuscript.

**Competing interests** The authors declare no competing interests.

### References

- Agrawal, S., Umapathy, S., & Dhiman, R. K. (2015). Minimal hepatic encephalopathy impairs quality of life. *J Clin Exp Hepatol*, 5(Suppl 1), 42–48. <https://doi.org/10.1016/j.jceh.2014.11.006>.
- Ahboucha, S., Layrargues, G. P., Mamer, O., & Butterworth, R. F. (2005). Increased brain concentrations of a neuroinhibitory steroid in human hepatic encephalopathy. *Annals of Neurology*, 58(1), 169–170. <https://doi.org/10.1002/ana.20534>.
- Bajaj, J. S., Schubert, C. M., Heuman, D. M., Wade, J. B., Gibson, D. P., Topaz, A., & Sanyal, A. J. (2010). Persistence of cognitive impairment after resolution of overt hepatic encephalopathy. *Gastroenterology*, 138(7), 2332–2340. <https://doi.org/10.1053/j.gastro.2010.02.015>.

- Butterworth, R. (2007). Neuronal cell death in hepatic encephalopathy. *Metabolic Brain Disease*, 22(3–4), 309–320. <https://doi.org/10.1007/s11011-007-9072-3>.
- Cauda, F., D'Agata, F., Sacco, K., Duca, S., Geminiani, G., & Vercelli, A. (2011). Functional connectivity of the insula in the resting brain. *Neuroimage*, 55(1), 8–23. <https://doi.org/10.1016/j.neuroimage.2010.11.049>.
- Cauli, O., Rodrigo, R., Llansola, M., Montoliu, C., Monfort, P., Piedrafitá, B., & Felipo, V. (2009). Glutamatergic and gabaergic neurotransmission and neuronal circuits in hepatic encephalopathy. *Metabolic Brain Disease*, 24(1), 69–80. <https://doi.org/10.1007/s11011-008-9115-4>.
- Chen, H. J., Zhu, X. Q., Shu, H., Yang, M., Zhang, Y., Ding, J., & Teng, G. J. (2012). Structural and functional cerebral impairments in cirrhotic patients with a history of overt hepatic encephalopathy. *European Journal of Radiology*, 81(10), 2463–2469. <https://doi.org/10.1016/j.ejrad.2011.10.008>.
- Chen, H. J., Jiang, L. F., Sun, T., Liu, J., Chen, Q. F., & Shi, H. B. (2015). Resting-state functional connectivity abnormalities correlate with psychometric hepatic encephalopathy score in cirrhosis. *European Journal of Radiology*, 84(11), 2287–2295. <https://doi.org/10.1016/j.ejrad.2015.08.005>.
- Chen, H. J., Liu, P. F., Chen, Q. F., & Shi, H. B. (2017). Brain microstructural abnormalities in patients with cirrhosis without overt hepatic encephalopathy: A voxel-based diffusion kurtosis Imaging Study. *Ajr. American Journal of Roentgenology*, 209(5), 1128–1135. <https://doi.org/10.2214/AJR.17.17827>.
- Cheng, Y., Zhang, G., Zhang, X., Li, Y., Li, J., Zhou, J., & Shen, W. (2021). Identification of minimal hepatic encephalopathy based on dynamic functional connectivity. *Brain Imaging Behav*, 15(5), 2637–2645. <https://doi.org/10.1007/s11682-021-00468-x>.
- Córdoba, J., & Mínguez, B. (2008). Hepatic encephalopathy. *Seminars in Liver Disease*, 28(1), 70–80. <https://doi.org/10.1055/s-2008-1040322>.
- Deen, B., Pitskel, N. B., & Pelphrey, K. A. (2011). Three systems of insular functional connectivity identified with cluster analysis. *Cerebral Cortex*, 21(7), 1498–1506. <https://doi.org/10.1093/cercor/bhq186>.
- Dhiman, R. K., & Chawla, Y. K. (2009). Minimal hepatic encephalopathy. *Indian Journal of Gastroenterology*, 28(1), 5–16. <https://doi.org/10.1007/s12664-009-0003-6>.
- Felipo, V. (2013). Hepatic encephalopathy: Effects of liver failure on brain function. *Nature Reviews Neuroscience*, 14(12), 851–858. <https://doi.org/10.1038/nrn3587>.
- Ferencik, P., Lockwood, A., Mullen, K., Tarter, R., Weissenborn, K., & Blei, A. T. (2002). Hepatic encephalopathy—definition, nomenclature, diagnosis, and quantification: Final report of the working party at the 11th World Congresses of Gastroenterology, Vienna, 1998. *Hepatology*, 35(3), 716–721. <https://doi.org/10.1053/jhep.2002.31250>.
- Häussinger, D., & Schliess, F. (2008). Pathogenetic mechanisms of hepatic encephalopathy. *Gut*, 57(8), 1156–1165. <https://doi.org/10.1136/gut.2007.122176>.
- Jones, E. A. (2000). Pathogenesis of hepatic encephalopathy. *Clinics in Liver Disease*, 4(2), 467–485. [https://doi.org/10.1016/s1089-3261\(05\)70119-7](https://doi.org/10.1016/s1089-3261(05)70119-7).
- Karanfilian, B. V., Park, T., Senatore, F., & Rustgi, V. K. (2020). Minimal hepatic encephalopathy. *Clinics in Liver Disease*, 24(2), 209–218. <https://doi.org/10.1016/j.cld.2020.01.012>.
- Keiding, S., & Pavese, N. (2013). Brain metabolism in patients with hepatic encephalopathy studied by PET and MR. *Archives of Biochemistry and Biophysics*, 536(2), 131–142. <https://doi.org/10.1016/j.abb.2013.05.006>.
- Lin, W., Chen, X., Gao, Y. Q., Yang, Z. T., Yang, W., & Chen, H. J. (2019). Hippocampal atrophy and functional connectivity disruption in cirrhotic patients with minimal hepatic encephalopathy. *Metabolic Brain Disease*, 34(6), 1519–1529. <https://doi.org/10.1007/s11011-019-00457-6>.
- Lin, S., Li, J., Chen, S., Lin, X., Ye, M., & Qiu, Y. (2021). Progressive Disruption of Dynamic Functional Network Connectivity in patients with Hepatitis B Virus-related cirrhosis. *Journal of Magnetic Resonance Imaging*, 54(6), 1830–1840. <https://doi.org/10.1002/jmri.27740>.
- Liu, K., Chen, G., Ren, S. Y., Zhu, Y. Q., Yu, T. L., Tian, P., & Yin, H. (2019). Regional gray matter abnormality in hepatic myelopathy patients after transjugular intrahepatic portosystemic shunt: A voxel-based morphometry study. *Neural Regen Res*, 14(5), 850–857. <https://doi.org/10.4103/1673-5374.249233>.
- Lockwood, A. H., Weissenborn, K., Bokemeyer, M., Tietge, U., & Burchert, W. (2002). Correlations between cerebral glucose metabolism and neuropsychological test performance in nonalcoholic cirrhotics. *Metabolic Brain Disease*, 17(1), 29–40. <https://doi.org/10.1023/a:1014000313824>.
- Menon, V., & Uddin, L. Q. (2010). Saliency, switching, attention and control: A network model of insula function. *Brain Struct Funct*, 214(5–6), 655–667. <https://doi.org/10.1007/s00429-010-0262-0>.
- Mesulam, M. M., & Mufson, E. J. (1982). Insula of the old world monkey. I. Architectonics in the insulo-orbito-temporal component of the paralimbic brain. *The Journal of Comparative Neurology*, 212(1), 1–22. <https://doi.org/10.1002/cne.902120102>.
- Mina, A., Moran, S., Ortiz-Olvera, N., Mera, R., & Uribe, M. (2014). Prevalence of minimal hepatic encephalopathy and quality of life in patients with decompensated cirrhosis. *Hepatology Research*, 44(10), E92–99. <https://doi.org/10.1111/hepr.12227>.
- Moran, S., López-Sánchez, M., Milke-García, M. D. P., & Rodríguez-Leal, G. (2021). Current approach to treatment of minimal hepatic encephalopathy in patients with liver cirrhosis. *World Journal of Gastroenterology*, 27(22), 3050–3063. <https://doi.org/10.3748/wjg.v27.i22.3050>.
- Ni, L., Qi, R., Zhang, L. J., Zhong, J., Zheng, G., Zhang, Z., & Lu, G. M. (2012). Altered regional homogeneity in the development of minimal hepatic encephalopathy: A resting-state functional MRI study. *PLoS One*, 7(7), e42016. <https://doi.org/10.1371/journal.pone.0042016>.
- Nomi, J. S., Farrant, K., Damaraju, E., Rachakonda, S., Calhoun, V. D., & Uddin, L. Q. (2016). Dynamic functional network connectivity reveals unique and overlapping profiles of insula subdivisions. *Human Brain Mapping*, 37(5), 1770–1787. <https://doi.org/10.1002/hbm.23135>.
- Ortiz, M., Jacas, C., & Córdoba, J. (2005). Minimal hepatic encephalopathy: Diagnosis, clinical significance and recommendations. *Journal of Hepatology*, 42(Suppl(1)), S45–53. <https://doi.org/10.1016/j.jhep.2004.11.028>.
- Qi, R., Xu, Q., Zhang, L. J., Zhong, J., Zheng, G., Wu, S., & Lu, G. (2012a). Structural and functional abnormalities of default mode network in minimal hepatic encephalopathy: A study combining DTI and fMRI. *PLoS One*, 7(7), e41376. <https://doi.org/10.1371/journal.pone.0041376>.
- Qi, R., Zhang, L., Wu, S., Zhong, J., Zhang, Z., Zhong, Y., & Lu, G. (2012b). Altered resting-state brain activity at functional MR imaging during the progression of hepatic encephalopathy. *Radiology*, 264(1), 187–195. <https://doi.org/10.1148/radiol.12111429>.
- Qi, R., Zhang, L. J., Xu, Q., Zhong, J., Wu, S., Zhang, Z., & Lu, G. (2012c). Selective impairments of resting-state networks in minimal hepatic encephalopathy. *PLoS One*, 7(5), e37400. <https://doi.org/10.1371/journal.pone.0037400>.
- Qi, R., Zhang, L. J., Xu, Q., Liang, X., Luo, S., Zhang, Z., & Lu, G. M. (2014). Abnormal functional connectivity within the default mode network in patients with HBV-related cirrhosis without hepatic encephalopathy revealed by resting-state functional MRI. *Brain Research*, 1576, 73–80. <https://doi.org/10.1016/j.brainres.2014.05.044>.

- Smith, R., Lane, R. D., Alkozei, A., Bao, J., Smith, C., Sanova, A., & Killgore, W. D. S. (2017). Maintaining the feelings of others in working memory is associated with activation of the left anterior insula and left frontal-parietal control network. *Soc Cogn Affect Neurosci*, *12*(5), 848–860. <https://doi.org/10.1093/scan/nsx011>.
- Stinton, L. M., & Jayakumar, S. (2013). Minimal hepatic encephalopathy. *Can J Gastroenterol*, *27*(10), 572–574. <https://doi.org/10.1155/2013/547670>.
- Tian, Y., & Zalesky, A. (2018). Characterizing the functional connectivity diversity of the insula cortex: Subregions, diversity curves and behavior. *Neuroimage*, *183*, 716–733. <https://doi.org/10.1016/j.neuroimage.2018.08.055>.
- Uddin, L. Q., Nomi, J. S., Hébert-Seropian, B., Ghaziri, J., & Boucher, O. (2017). Structure and function of the human insula. *Journal of Clinical Neurophysiology*, *34*(4), 300–306. <https://doi.org/10.1097/wnp.0000000000000377>.
- Wang, Y., Yang, X., Xiao, L., Li, W., Huo, X., Wang, C., & Sun, T. (2022). Altered anterior insula-superior frontal gyrus functional connectivity is correlated with cognitive impairment following total sleep deprivation. *Biochemical and Biophysical Research Communications*, *624*, 47–52. <https://doi.org/10.1016/j.bbrc.2022.07.078>.
- Yang, Z. T., Chen, H. J., Chen, Q. F., & Lin, H. (2018). Disrupted brain intrinsic networks and executive dysfunction in cirrhotic patients without overt hepatic encephalopathy. *Frontiers in Neurology*, *9*, 14. <https://doi.org/10.3389/fneur.2018.00014>.
- Zhang, L. J., Zheng, G., Zhang, L., Zhong, J., Wu, S., Qi, R., & Lu, G. (2012). Altered brain functional connectivity in patients with cirrhosis and minimal hepatic encephalopathy: A functional MR imaging study. *Radiology*, *265*(2), 528–536. <https://doi.org/10.1148/radiol.12120185>.
- Zhang, L. J., Zheng, G., Zhang, L., Zhong, J., Li, Q., Zhao, T. Z., & Lu, G. M. (2014). Disrupted small world networks in patients without overt hepatic encephalopathy: A resting state fMRI study. *European Journal of Radiology*, *83*(10), 1890–1899. <https://doi.org/10.1016/j.ejrad.2014.06.019>.
- Zhang, W., Ning, N., Li, X., Li, M., Duan, X., Guo, Y., & Yang, J. (2019). Impaired brain glucose metabolism in cirrhosis without overt hepatic encephalopathy: A retrospective 18F-FDG PET/CT study. *Neuroreport*, *30*(11), 776–782. <https://doi.org/10.1097/wnr.0000000000001284>.

**Publisher's Note** Springer Nature remains neutral with regard to jurisdictional claims in published maps and institutional affiliations.

Springer Nature or its licensor (e.g. a society or other partner) holds exclusive rights to this article under a publishing agreement with the author(s) or other rightsholder(s); author self-archiving of the accepted manuscript version of this article is solely governed by the terms of such publishing agreement and applicable law.